Psychoacoustic analysis of contra-rotating propeller noise for Unmanned Aerial Vehicles

Antonio J. Torija,[1] [a] Paruchuri Chaitanya,[2,] and Zhengguang Li[3]

[1] *Acoustics Research Centre, University of Salford, Manchester, M5 4WT, United Kingdom*

[2] *Institute of Sound and Vibration Research, University of Southampton, Southampton, SO17 1BJ, United Kingdom*

[3] *Department of Architecture, Zhejiang University of Science and Technology, Hangzhou, 310023, P.R. China*

Unmanned aerial vehicle (UAV) technologies are rapidly advancing due to the unlimited number of applications from parcel delivery to people transportation. As the UAV market expands, community noise impact will become a significant problem for public acceptance. Compact drone architectures based on contra-rotating propellers bring significant benefits in terms of aerodynamic performance and redundancy to ensure vehicle control in case of component failure. However, contra-rotating propellers are severely noisy if not designed appropriately. In the framework of a perception-influenced design approach, this paper investigates the optimal rotor spacing distance configuration to minimise noise annoyance. On the basis of a series of psychoacoustic metrics (i.e. loudness, fluctuation strength, roughness, sharpness and tonality) and psychoacoustic annoyance models, the optimal rotor axial separation distance (expressed as a function of propeller blade diameter) is at a range of 0.2 to 0.4. This paper also discusses the performance of currently available psychoacoustic models to predict propeller noise annoyance, and defines further work to develop a psychoacoustic annoyance model optimised for rotating systems.

[a] A.J.TorijaMartinez@salford.ac.uk

I. INTRODUCTION

New aviation markets, such as Urban Air Mobility (UAM) operations for passengers and drone operations for goods' deliveries and blue light services, are estimated to have a global potential of between $132 and $227 billion over the next 20 years (ATI, 2019). As the drone delivery market intensifies over the coming years, the payload requirement is predicted to increase by a factor of 50 to 100, leading to further problems with their public acceptance; with noise becoming a primary focus. This increase in payload requirements can only be achieved with compact drone architectures such as co-axial or overlapping propellers. The use of contra-rotating propellers in Unmanned Aerial Vehicles (UAVs) has the benefit of increasing aerodynamic performance (Stract et al., 1981), reducing the UAV's plan size and adding redundancy in case of component failure (McKay et al., 2019).

However, the small tip-to-tip spacing between contra-rotating propellers results in a significant source of noise due to blade interaction effects (Tinney and Sirohi, 2018; Alexander et al., 2019). Extensive laboratory testing has found that in the frequency spectra of multi-rotor UAV there are significant sound levels at higher harmonics of the blade passage frequency, which seems to be caused by interaction noise from disturbed inflow due to other rotor blades or the fuselage (Magliozzi, 1991; Cabell et al., 2016; Torija et al., 2019). In an experimental investigation of static multi-rotor contra-rotating UAV propellers, McKay et al. (2019) observed that potential field interaction tones are about 20 dB higher than rotor alone tones at typical ground observer locations with a hovering UAV. This suggests that proper design of multi-rotor contra-rotating UAV propellers to minimise interaction between rotors can lead to significant reductions in noise emission.

The noise sources on a co-axial propeller system can be categorized into either rotor self-noise or interaction noise. Rotor self-noise is principally composed of tonal components and has contributions due to the steady loading and aerofoil thickness, while the broadband component is relatively weak (Marte and Kurtz, 1970). An interaction source is generated when the spiraling wake and tip vortex

from the upper propeller interacts with the lower propeller. At sufficiently small rotor separation distances, an additional interaction noise source is present arising from the interaction of the potential near field of each propeller with the other (Heff, 1990). A more recent study by Chaitanya et al. (2020) performed a detailed investigation on the sensitivity of the aerodynamic and aeroacoustic performance to the axial separation distance between a counter-rotating propeller configuration. An optimum separation distance to diameter ratio for maximum efficiency and minimum radiated noise was found to be at 0.25 based on overall sound power level. The reason behind this optimum is attributed to the balance between potential field interactions and tip-vortex interactions radiated from the contra-rotating configuration. The current paper extends their work to perform psychoacoustic optimization of contra-rotating propellers.

Anghinolfi et al. (2016) carried out a psychoacoustic optimization of blade spacing in subsonic, open, or nearly open axial-flow rotors. This optimization focused only on tonal noise and the objective function was based on the Tone-to-Noise Ratio (TNR) metric. They found optimal blade spacing for different numbers of blade rotors as a function of TNR and level of the highest tonal peak. However, these results do not have direct relation to loudness or other psychoacoustic features.

The perception-influenced design approach (Rizzi, 2016) aims to incorporate human response into the process of creating low-noise aircraft. Metrics that correlate well with human response to noise can potentially be incorporated into the aircraft design cycle to effectively reduce community noise impact (Krishnamurthy et al., 2018). Current noise certification metrics do not necessarily reflect the characteristics of noise signatures of unconventional aircraft designs (Rizzi, 2016; Christian and Cabell, 2017; Torija et al., 2019), and therefore may not be able to predict human response. Torija et al. (2019) found that the Effective Perceived Noise Level (EPNL) is unable to account for the perceptual effect of series of complex tones spaced evenly across the frequency spectrum with relatively even sound levels, which is typical of multi-rotor vehicles (Cabell et al., 2016; Torija et al.,

2019). Other metrics, such as the Sound Exposure Level (SEL), do not account for the effects of tonal noise, which is a major contributor towards the perceived annoyance due to aircraft noise (Angerer et al., 1991; Berckmans et al., 2008; More, 2011; White et al., 2017). Therefore, the use of current noise certification metrics for aircraft design might lead to suboptimal solutions.

Psychoacoustic metrics have been widely applied to improve the sound quality of different consumer products, especially in the automotive industry (Lyon, 2003). Psychoacoustic metrics, such as loudness, sharpness, tonality, roughness and fluctuation strength, are good indicators of how the human auditory system reacts to different features of acoustic stimuli (Zwicker and Fastl, 1999). Loudness measures the sensation of sound intensity. Sharpness and tonality describe the perceptual effects of spectral imbalance of the sound towards the high frequency region, and the presence of spectral irregularities or tones respectively. Fluctuation strength and roughness describe how slow and rapid fluctuations, respectively, of the sound level are perceived. The psychoacoustic metrics sharpness, tonality and fluctuation strength have been suggested as good indicators of rotorcraft noise annoyance (Krishnamurthy et al., 2018; Boucher et al., 2020). Investigating the performance of different psychoacoustic metrics to account for the perception of different aspects of aircraft noise, Barbot et al. (2008) found fluctuation strength as a good indicator of perceptual effects of turbulence and sharpness as a good indicator of the perceptual effects of high frequency noise. Torija et al. (2019) found that Aures/Terhardt tonality (Aures, 1985b) improves on the EPNL Tone Correction in terms of accounting for the presence of complex tones in aircraft noise.

Perception of mechanical sounds is a complex process due to the amount of noise features involved (e.g. tonal components, amplitude modulated sounds, etc.). To address this issue, Zwicker and Fastl (1999) proposed a model for combining several psychoacoustic metrics into one model to quantify annoyance (hereinafter called Zwicker's model for short). Using the Zwicker's psychoacoustic annoyance (PA) model, relative annoyance degrees of different noise samples can be estimated from

measures of loudness, sharpness, fluctuation strength and roughness. However, Zwicker's PA model does not include a factor accounting for the influence of the tonality on noise annoyance. To improve accuracy in the estimation of relative annoyance degrees caused by several types of tonal/atonal noises, Di et al. (2016) carried out an update of Zwicker's PA model aiming at tonal noises. More (2011) developed a modified version of Zwicker's PA model based on the results of seven psychoacoustic tests for several aircraft sounds with varying psychoacoustic parameters. The modified PA model developed by More, which includes a term based on Aures/Terhardt tonality and loudness to account for the perceptual effect of tonal noise, was found able to accurately predict aircraft noise annoyance.

The aim of this paper is to perform a psychoacoustic analysis of a single static contra-rotating propeller mounted in an anechoic chamber. A set of psychoacoustic metrics are calculated for a series of far-field microphone measurements with different separation distance between the contra-rotating propellers. The contribution of each noise source component on the co-axial propeller under study is evaluated from a perceptual standpoint, using relevant psychoacoustic metrics. Working towards the development of a framework for the psychoacoustic optimisation of novel aerial vehicles, this paper investigates the optimal distance between contra-rotating propellers to minimise psychoacoustic impact. The performance of PA models to predict noise annoyance for propeller systems is evaluated and discussed. The main assumption in this paper is that PA models optimized for propeller noise annoyance can be used to inform propeller design for lower psychoacoustic impact.

This paper is structured as follows: Section II describes the experimental setup for acoustic measurements and the metrics for psychoacoustic analysis; Section III presents and discusses the experimental results and are followed by the main conclusions of this work in section IV.

II. EXPERIMENTAL AND PSYCHOACOUSTIC METHODS

A. Experimental set-up and procedure

The overlapping rotor test rig designed and manufactured at the University of Southampton consisted of two FOXTECH W61-35 brushless DC (BLDC) (16 poles) 700W motors mounted on a carbon fibre beam as shown in Fig. 1. A commercially available T-Motor 16 inch 5.4 inch rotor was used for this overlapping rotor propulsion system analysis. Two Hyperion HP-EM2-TACHBL sensors were used to measure the precise Rotations Per Minute (RPM). Two Maytech 40A-OPTO speed controllers were used to accurately control the BLDC motors. The overlapping rig allowed manipulation of the propulsion system in both rotor horizontal separation distance d/D (with D as the rotor diameter) and rotor axial separation distance z/D. z/D rotor separation was achieved by a custom linear actuator traversing the upper rotor. All of the tests for this study were achieved when the lower rotor plane was at least three rotor diameters away from the ground with anechoic wedges beneath. The selected lead screw and stepper motor configuration allows for z/D variations varying of 0.05 to 1. Sixteen z/D positions were tested: 0.05, 0.075, 0.1, 0.125, 0.15, 0.175, 0.2, 0.25, 0.3, 0.35, 0.4, 0.45, 0.5, 0.6, 0.8 and 1. The combined thrust of the dual-rotor propulsion system is varied from 2 to 20N in steps of 2N. Although 10 thrust settings were measured, the results shown in this paper refer to a thrust of 10 N (varying thrusts lead to changes in magnitudes, but do not alter the trends shown below). A detailed description of the rig is presented by Brazinskas (2019).

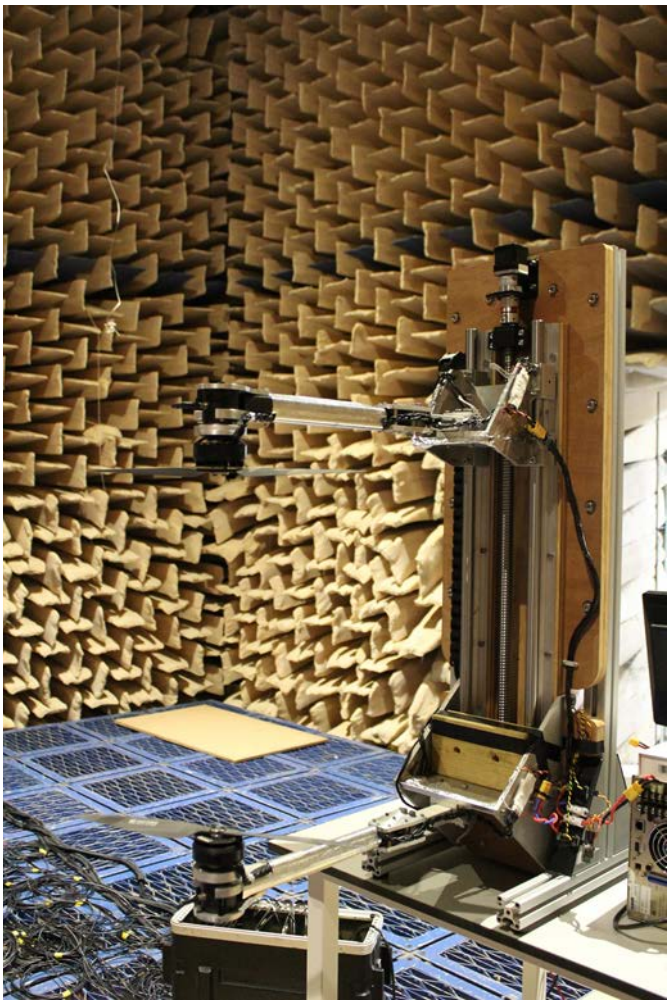

FIG. 1. (Color online). Photograph of overlapping propeller rig within the anechoic chamber of the Institute of Sound and Vibration Research at the University of Southampton.

B. Far-field noise measurements

The overlapping far-field noise measurements were carried out at the Institute of Sound and Vibration Research's open-jet wind tunnel facility. The overlapping rotor test rig was located within an anechoic chamber, of dimension 8 m × 8 m × 8 m as shown in Fig. 1. The walls, acoustically treated with glass wool wedges, allow a cut-off frequency of 80 Hz.

Far-field noise measurements were made using 10, ½ in. condenser microphones (B&K type 4189) located at a constant radial distance of 2.5 m from the centre of the propellers. These microphones were placed at emission angles of between 12 and 102 degrees measured relative to the bottom

propeller. Measurements were carried out for 10 s duration at a sampling frequency of 50 kHz, and the noise spectra was calculated with a window size of 1024 data points corresponding to a frequency resolution of 48.83 Hz and a Bandwidth-Time (BT) product of about 500, which is sufficient to ensure negligible variance in the spectral estimated at this frequency resolution. Please note that the data analysed in this paper is same as the data presented in Chaitanya et al. (2020).

C. Psychoacoustic data analysis

Unlike physical quantities (e.g. sound pressure level), psychoacoustic metrics provide a linear representation of human hearing perception (HEAD Acoustics, 2018). Psychoacoustic metrics have been found to outperform conventional noise metrics (e.g. EPNL or SEL) in predicting noise annoyance of fixed-wing aircraft (Rizzi et al., 2016; Torija et al., 2019). Recently, several authors (Krishnamurthy et al., 2018; Boucher et al., 2020) have explored the potential of psychoacoustic metrics for the modelling of human annoyance to rotorcraft noise, and assessed the performance of each psychoacoustic metric to account for rotorcraft noise annoyance response.

The psychoacoustic metrics (including loudness in sone, sharpness in acum, fluctuation strength in vacil, roughness in asper, impulsiveness in IU, and tonality in TU) of all sound samples were calculated with ArtemiS software (HEAD acoustics GmbH). Loudness was calculated according to DIN 45631/A1 (2010), which is based on Zwicker loudness model and includes a modification for time varying signals. The calculation of sharpness was made according to the standard DIN 45692 (2009). This sharpness method does not take into account the influence of absolute loudness on the sharpness perception. There are no standard methods for calculating roughness and fluctuation strength. These two metrics were calculated according to the hearing model given by Sottek (1993). Sottek's hearing model simulates the signal processing of human hearing and accounts for its limitations to track fast temporal changes within a critical band (Boucher et al., 2020). Tonality was calculated according to Aures/Terhardt tonality model (Aures, 1985b).

147 Three PA models were implemented to discuss their performance in assessing propeller noise
148 annoyance. The Zwicker PA model, accounting for the relation between annoyance and hearing
149 sensations loudness (*N*), sharpness (*S*), fluctuation strength (*F*) and roughness (*R*) is given by

150 $$PA = N_5\left(1 + \sqrt{w_S^2 + w_{FR}^2}\right) \quad (1)$$

151 where

152 N_5 is the 5th percentile of the loudness (in sone)

153 $$w_S = \{(S - 1.75)\cdot 0.25\lg(N_5 + 10),\ S > 1.75;\ 0,\ S \le 1.75\} \quad (2)$$

154 $$W_{FR} = \frac{2.18}{N_5^{0.4}}(0.4F + 0.6R) \quad (3)$$

155 Note that although non specified by Zwicker in the original form of eq. 1, the 5th percentiles of
156 sharpness, fluctuation strength and roughness metrics were used for calculating PA.

157 The use of 5th percentiles in psychoacoustic analysis is a standard approach widely accepted in the
158 literature. However, these percentile values are dependent on the recording time and the fluctuation
159 of the psychoacoustic parameter in question. This makes that the 5th percentile values for
160 psychoacoustic metrics cannot be compared without appropriate background information. In this
161 research, there is a steady sound pressure during the 10 s duration of each sound sample analysed.
162 For instance, the 5th percentile and arithmetic mean of the loudness for the rotor spacing z/D = 0.05
163 at azimuthal angle = 12 degrees is 98.5 and 96.4 sones respectively. Therefore, the findings of this
164 research can be argued to be non-dependent of the statistical parameters used to describe the
165 psychoacoustic magnitudes. Furthermore, to avoid the transient effect of the digital filters (used for
166 the computation of the psychoacoustic metrics evaluated) at the start of the audio signal analysis, the

first 0.5 s of the sound sample was ignored in the calculation of the 5th percentile of each psychoacoustic metric.

As described above, the Zwicker's PA model does not include a factor for accounting for the perceptual effects of tonal sounds. Di et al. (2016) derived a tonality factor (eq. 5) to develop a PA model able to account for the annoyance response of sounds with strong tonal components. The updated PA model developed by Di et al. (2016) (PA') is given by

$$PA' = N_5\left(1 + \sqrt{w_S^2 + w_{FR}^2 + w_T^2}\right) \tag{4}$$

where

$$w_T = \frac{6.41}{N_5^{0.52}}T \tag{5}$$

More (2011) developed a modified version of Zwicker PA model optimised to predict aircraft noise annoyance. The More's PA model (PA_{mod}) is given by

$$PA_{mod} = N_5\left(1 + \sqrt{\gamma_0 + \gamma_1 w_S^2 + \gamma_2 w_{FR}^2 + \gamma_3 w_T^2}\right) \tag{6}$$

where

$$w_T^2 = [(1 - e^{-\gamma_4 N_5})^2 \cdot (1 - e^{-\gamma_5 T})^2] \tag{7}$$

The estimates for the More's PA model were optimised for aircraft noise on the basis of a series of psychoacoustic tests. The value of these estimates for eqs. 6 and 7, i.e. $\gamma_0 = -0.16, \gamma_1 = 11.48, \gamma_2 = 0.84, \gamma_3 = 1.25, \gamma_4 = 0.29$ and $\gamma_5 = 5.49$, show the significant emphasis of the More's PA model on sharpness and tonality. Note that 5th percentile of Aures/Terhardt tonality was used for calculating PA in Di et al.'s and More's models.

None of these PA models account for the impulsiveness of the audio signal. Although there is no agreement in the literature, some authors advise that the prevalence of annoyance due to rotorcraft is influenced by its impulsiveness (Mestre et al., 2017). The impulsiveness (measured in IU) of all sound samples were calculated using the Sottek's hearing model. This psychoacoustic metric accounts for the perception caused by short and sudden changes in sound pressure level (Boucher, et al., 2019). A full description of the calculation of the impulsiveness metrics and its computation in the Sottek's hearing model can be found at Sottek et al. (1995) and Sottek and Genuit (2005) respectively. McMullen (2014) suggested that a combination of different psychoacoustic metrics, including loudness, sharpness, tonality and impulsiveness might provide an accurate assessment of human response to helicopter noise. All this suggests that impulsiveness might need to be considered for developing a PA model for rotorcraft noise.

III. RESULTS AND DISCUSSION

A. Directivity and spectra patterns

Figure 2 shows the 5th percentile of loudness (Fig. 2C) and sharpness (Fig. 2D) as a function of azimuthal angle (i.e. emission angles between 12 and 102 degrees measured relative to the rotor axis), for rotor spacings z/D=0.05, 0.2 and 1 and a thrust setting of 10 N. Maximum noise emission (i.e. loudness) is found at the rotor axis. Loudness decreases with azimuthal angle, reaching minimum values at 82-92 degrees (Fig. 2C). The same directivity pattern is observed for all rotor spacing evaluated. This is consistent with Chaitanya et al.'s (2020) previously observed optimum separation distance based on overall sound power level (see Figs. 2A and 2B for equivalent sound pressure level (SPL) and equivalent A-weighted SPL as a function of emission angle). Equivalent SPL, equivalent A-weighted SPL and loudness are lower at rotor spacing z/D=0.2 than at rotor spacings z/D=0.05 and z/D=1.

For all rotor spacings, maximum values of sharpness are observed at azimuthal angles of 82 to 92 degrees (Fig. 2D). Sharpness at rotor spacing z/D=0.2 is higher than sharpness at rotor spacings z/D=0.05 and z/D=1. Directivity patterns of loudness and sharpness metrics seem to be in line with the initial hypothesis that the highest contribution to measured sounds is the noise emission of potential field interaction tones. McKay et al. (2019) found that potential field interaction tones in co-axial propellers have a dipole directivity with a null at 90 degrees. In this research, the dip in the value of equivalent SPL, equivalent A-weighted SPL and loudness at about 82-92 degrees (as shown in Figs. 2A, 2B and 2C) can be attributable to a decline in the noise emission of potential field interaction tones. As the coaxial distance between the two contra-rotating propellers was varied during this experimentation, it was decided to position the 10 microphones (see Section II) at azimuthal angles relative to the bottom propeller (see Fig. 1). Hence, the slight shift in the dip of noise radiation from 90 degrees to 82 degrees. However, more work is required to better understand directivities of contra-rotating propellers due to the numerous noise sources involved (Chaitanya et al., 2020).

The decline in amplitude of potential field interaction tones at about 82-92 degrees also leads to an important increase in the relative contribution of higher harmonics of the blade passage frequencies (BPFs) and high frequency broadband noise, which is accounted for by an increase of sharpness as shown in Fig. 2D.

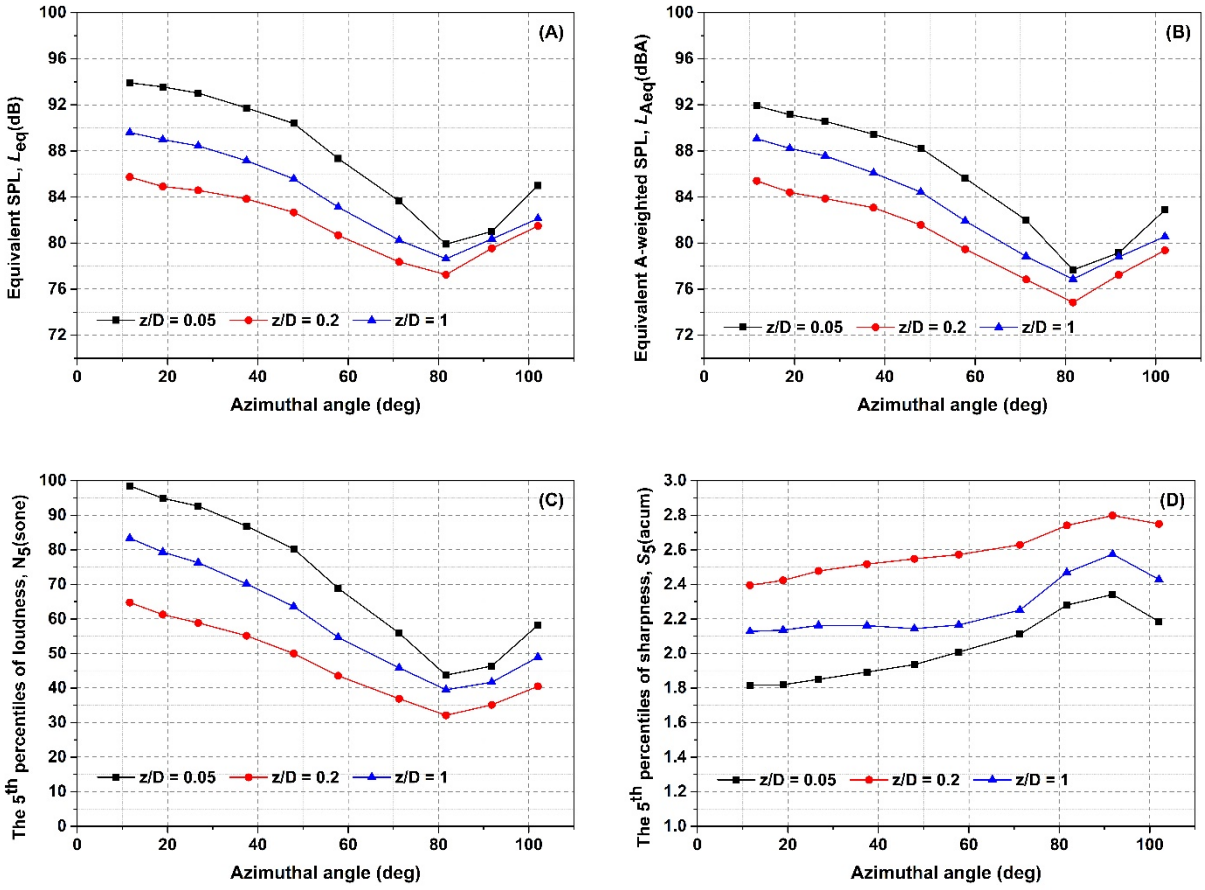

FIG. 2. (Color online). The equivalent SPL (A), equivalent A-weighted SPL (B), and the 5th percentiles of loudness (C) and sharpness (D) as a function of azimuthal angle, for a thrust setting of 10 N and for rotor spacings z/D=0.05, 0.2 and 1.

To continue with the investigation of the individual noise sources in the contra-rotating propeller under study, a narrow band frequency analysis was conducted. Figure 3 shows the narrow band frequency spectra for the rotor spacings z/D=0.05, 0.2 and 1 for azimuthal angles 12 deg (Fig. 3A) and 82 deg (Fig. 3B), and a thrust setting of 10 N. These two azimuthal angles allow the comparison between the narrow band frequency spectra for high loudness (i.e. 12 deg) and high sharpness (i.e. 82 deg).

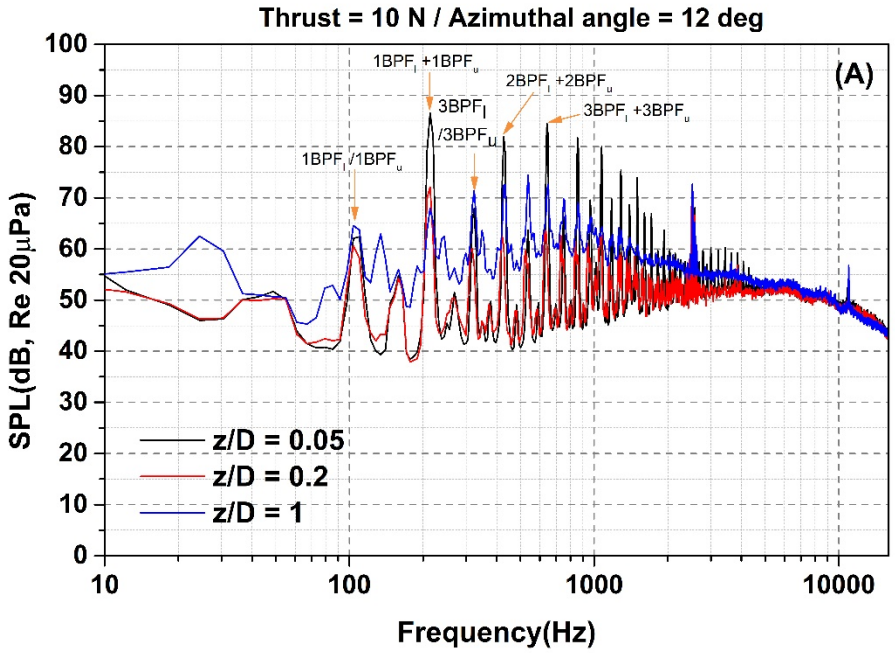

240

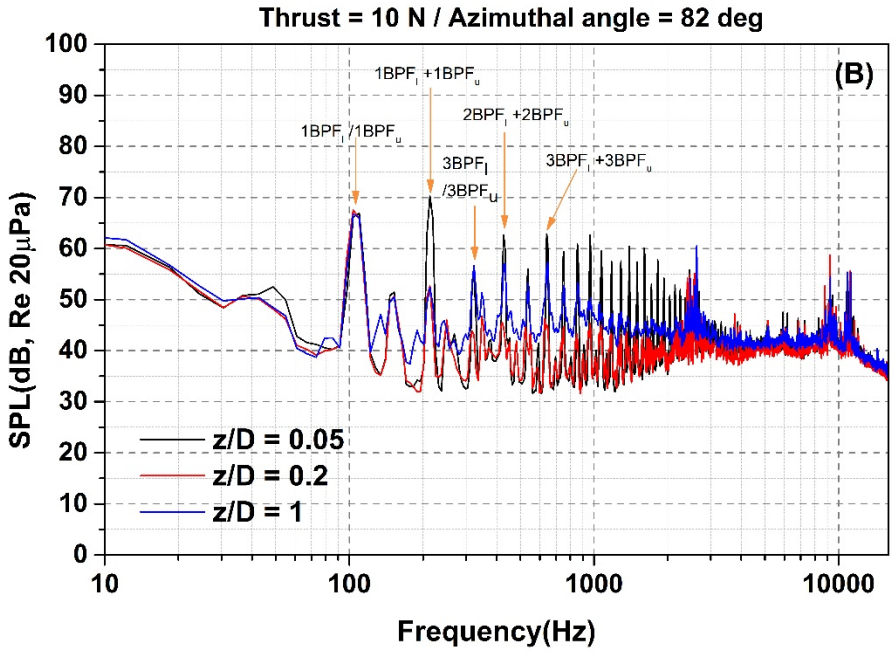

241

242 FIG. 3. (Color online). Narrow band frequency spectra for the rotor spacings z/D=0.05, 0.2 and 1
243 for a thrust setting of 10 N, and for azimuthal angles 12 deg (A) and 82 deg (B). Note that BPF_l and
244 BPF_u are the Blade Passing Frequencies (BPFs) of the lower and upper propeller respectively; and

245 $nBPF_l$ and $nBPF_u$ are their harmonics. Also shown the dominant potential field interaction tones
246 ($nBPF_l + nBPF_u$).

247 As shown in Fig. 3, the noise signatures of the contra-rotating propeller measured are dominated
248 by tonal components distributed along the frequency spectrum (between 0.1 and 2 kHz). These tonal
249 components include potential field interaction tones at frequencies that are the summation of rotor
250 BPFs. Fig. 3 displays the BPFs of the lower and upper propeller respectively, and their harmonics
251 ($nBPF_l$ and $nBPF_u$); and also, the dominant potential field interaction tones ($nBPF_l + nBPF_u$). An
252 analysis carried out by McKay et al. (2019) and Chaitanya et al. (2020) demonstrated that interaction
253 tones are predominantly caused by potential field interactions, and therefore, they decay rapidly with
254 rotor spacing. This decay in amplitude of potential field interaction tones is observed by comparing
255 frequency spectra of rotor spacings z/D=0.05 and 0.2. The decrease in amplitude of potential field
256 interaction tones as rotor spacing increases, leads to a sound signature with higher relative contribution
257 of high frequency components (broadband and tonal components over 2 kHz). As the rotor spacing
258 continues increasing, from z/D=0.05 and 0.2 to z/D=1, the contribution of broadband noise
259 increases. This increase can be attributed to the enhanced interaction between the turbulence
260 generated by the upper propeller tip vortex and the lower propeller as demonstrated by Chaitanya et
261 al. (2020).

262 At an emission angle of 82 degrees, the amplitude of potential field interaction tones significantly
263 decays (especially for rotor spacing z/D=0.2), due to their dipole directivity (as described above). A
264 decrease of about 20 dB is observed in the amplitude of potential field interaction tones at 82 degrees
265 compared to the amplitude at 12 degrees (see Fig. 3). For the specific case of rotor spacing z/D=0.05
266 at 82 degrees, the amplitude of potential field interaction tones is of the same order of magnitude as
267 the amplitude of BPF tones (Fig. 3B). This is due to both the dipole directivity of potential field
268 interaction tones with a null at about 90 degrees and the maximum emission of BPF tones in the plane

of the propeller (McKay et al., 2019). At an emission angle of 82 degrees there is a reduction of high frequency broadband noise (compared to 12 degrees), and a series of tonal components of important magnitude are observed in the high frequency region, i.e. 2-12kHz. The precise reason for this behaviour is currently not known and more work is required to understand this phenomenon.

B. Psychoacoustic metrics vs. rotor spacing

To investigate the optimum rotor spacing configuration for the contra-rotating system under study, the value of the different psychoacoustic metrics described above in Section II.C has been calculated. The value of psychoacoustics metrics (5^{th} percentile) as a function of rotor spacing at an azimuthal angle of 12 and 82 degrees is shown in Fig. 4. As described above (Section III.A), at 12 and 82 degrees the contra-rotating system measured has the highest and lowest noise emission respectively.

As the rotor spacing increases, the amplitude of the potential field interaction tones distributed along the mid to high frequency regions decays significantly (see Fig. 3). Consequently, as shown in Fig. 4A, loudness decreases with an increase in rotor spacing, reaching the lowest values at the region z/D=0.2-0.4 at 12 degrees and z/D=0.2-0.3 at 82 degrees. This decay is more significant at 12 degrees (about 30 sone reduction between rotor spacings z/D=0.05 and 0.2) where the emission of potential field interaction tones is maximum, compared to 82 degrees (about 10 sone reduction between rotor spacings z/D=0.05 and 0.2). At small rotor spacings, the decrease in loudness is due to a reduction in the potential field interactions between the two contra-rotating propellers. This interaction noise is primarily tonal, and hence tonality drops significantly as rotor spacing increases (see Fig. 4B). These results are in line with existing literature (McKay et al., 2019; Chaitanya et al., 2020), where blade spacing optimization has been demonstrated to lead to important reductions in tonal noise (Anghinolfi et al., 2016). Figure 4B shows that, at 12 degrees, there is a significant drop in tonality at a rotor spacing z/D=0.35, to remain almost constant regardless rotor spacing onwards. At 82 degrees, this significant drop in tonality is found at a rotor spacing z/D=0.2 (Fig. 4B). This might be due to the

directivity characteristics of potential field interactions, as described in Section III.A. With higher amplitude of potential field interaction tones at emission angles about 0 degrees relative to the rotor axis, a greater rotor spacing is needed at 12 degrees for tonality to drop to minimum values (compared to 82 degrees). At both emission angles, 12 and 82 degrees the same minimum value of tonality is observed at a rotor spacing z/D=0.35 (Fig. 4B).

Fluctuation strength accounts for the low frequency amplitude modulation consequence of the closely spaced potential field interaction tones, as shown in Fig. 3. As rotor spacing increases beyond z/D=0.15-0.2, potential field interactions are reduced (i.e. amplitude of interaction tones decays), and consequently a significant drop in fluctuation strength is observed (Fig. 4C).

With increase in rotor separation distances, interaction noise between rotors increases due to enhanced turbulence-propeller interactions because of unsteadiness in the tip vortex as previously demonstrated by Chaitanya et al. (2020). This added turbulence-propeller interaction noise, which is tonal and broadband in nature (see Fig. 3), causes an increase of loudness after rotor spacing z/D=0.4 (Fig. 4A). Modulated broadband noise reaches higher roughness values than modulated discrete tones, and even unmodulated broadband noise attains considerable roughness values due to random envelope fluctuations (Daniel, 2008). Therefore, the increase in unsteady turbulence-propeller interaction noise as rotors are moved apart might explain the gradual growth of roughness shown in Fig. 4D. At 12 degrees, the highest emission of broadband noise due to unsteady turbulence-propeller interaction noise leads to a higher rate of increase in roughness with rotor spacing (as observed in Fig. 4D).

As seen in Fig. 4E, impulsiveness significantly increases as the rotor spacing grows. This is observed for both azimuthal angles of highest and lowest noise emission, although the highest values of impulsiveness are at 12 degrees. As discussed by Krishnamurthy et al. (2018), impulsiveness and roughness metrics are strongly linked to each other. This is observed in this paper by comparing Figs.

4D and 4E. Noise caused by enhanced turbulence-propeller interactions is highly impulsive, and therefore, the added turbulence-propeller interaction noise as the contra-rotating rotors move apart from each other leads to an increase in the impulsiveness metric. This suggests that the impulsiveness metric should be considered, along with roughness, to account for the perceptual response to propeller-turbulence interaction noise in the development of a PA model for rotorcraft noise.

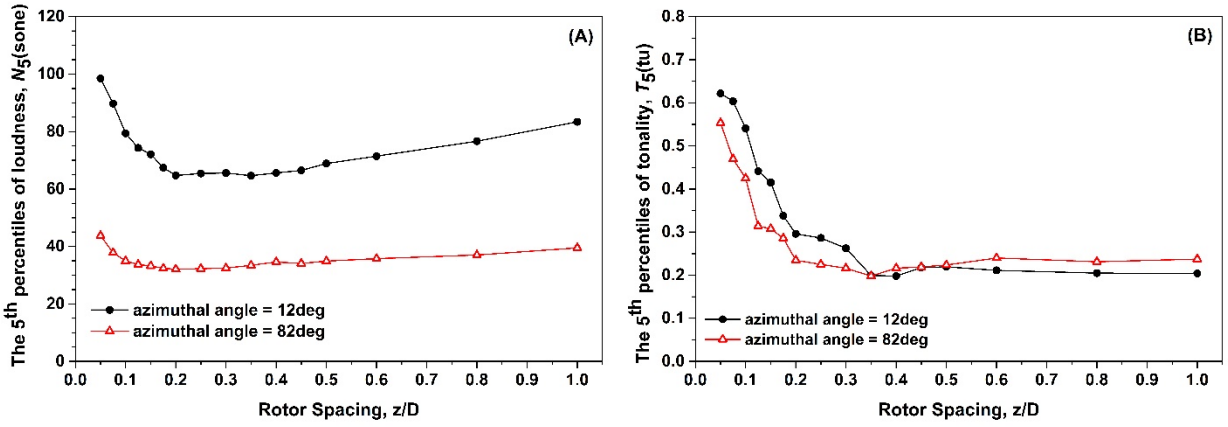

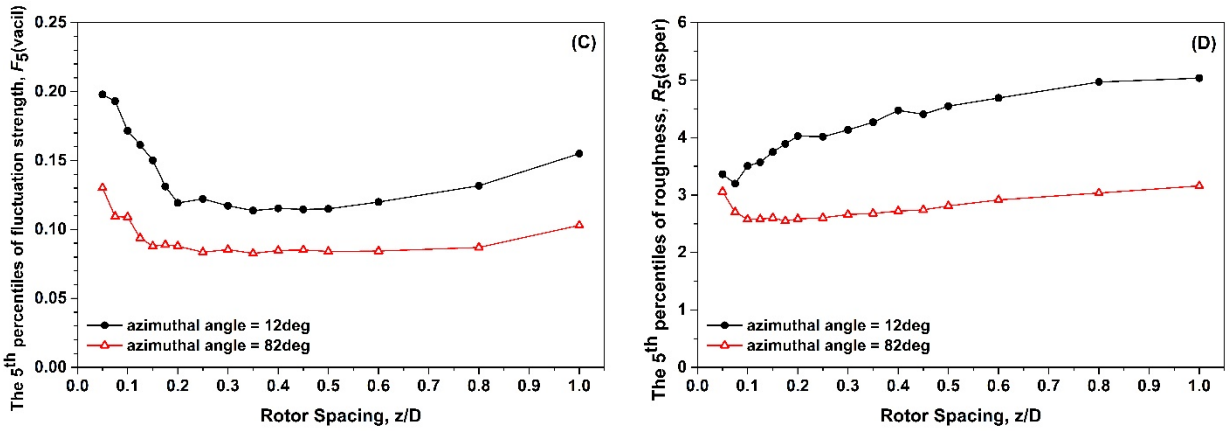

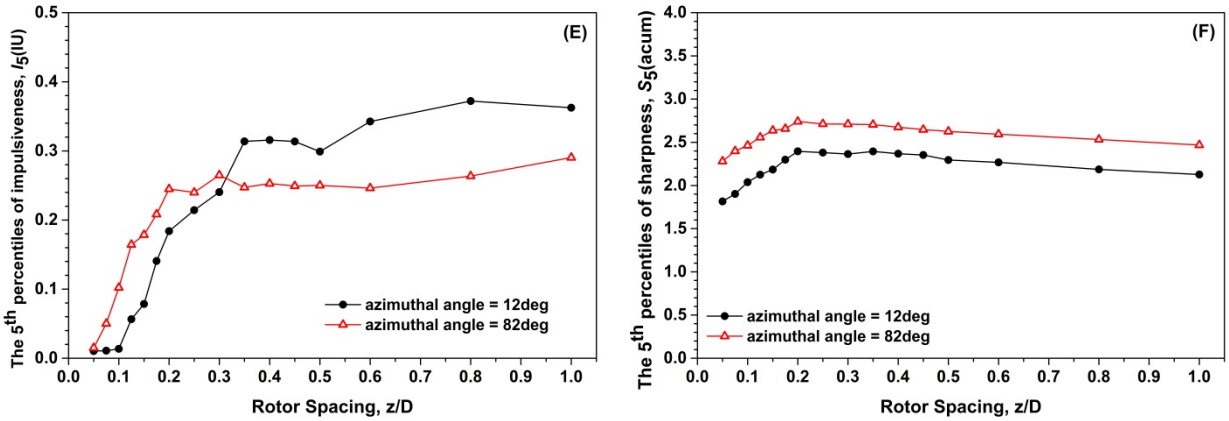

FIG. 4. (Color online). The 5th percentiles of loudness (A), tonality (B), fluctuation strength (C), roughness (D), impulsiveness (E) and sharpness (F) as a function of rotor spacing at azimuthal angle12 deg and 82 deg, for a thrust setting of 10 N.

At rotor spacings in the region z/D=0.2-0.4, the contribution of potential field interaction tones reaches a minimum. This leads to an increase in the relative contribution of high frequency tonal and broadband components (i.e. shaper sounds). Therefore, at rotor spacings z/D=0.2-0.4, the spectral centroid is located at a higher frequency (compared to audio signals of rotor spacings with dominant potential field interaction tones), and therefore higher values of sharpness are observed (Fig. 4F). The same pattern of sharpness as a function of rotor spacing is observed for both 12 and 82 degrees, although sharpness values are higher at 82 degrees due to the lowest emission of potential field interaction tones at these emission angles. Cabell et al. (2016) found important emissions of high frequency tones between 3.5 and 5 kHz for a series of multi-copters driven by brushless DC motors. The noise generated by brushless DC motors is primarily due to both force pulses as the magnets and armature interact and forces caused by phase changes in the motor drive signal (Brackley and Pollock, 2000). Alexander at al. (2019) observed high frequency humps in a series of multi-copters measured at hover configuration. Although the authors state this noise being broadband in nature, its origin is still under investigation.

C. Models for psychoacoustic annoyance

To identify the optimal rotor spacing configuration for the contra-rotating propeller under evaluation, PA as a function of rotor spacing has been calculated according to PA models developed by Zwicker and Fastl (1999), Di et al. (2016) and More (2011). As shown in Fig. 5, as expected from the value of the psychoacoustic metrics analysed in section III.B, the lowest values of PA are found for rotor spacing in the rage of z/D=0.2-0.4 for both 12 and 82 degrees.

At 12 degrees, i.e. the emission angle with the highest amplitude of potential field interaction tones, three main results are observed in Fig. 5A: (i) A significant decay in PA is observed at the optimal rotor spacing area, compared to rotor spacings below z/D=0.2 and above z/D=0.4. (ii) As rotor interaction noise at this rotor spacing is tonal in nature (i.e. potential field interaction tones), Di et al.'s PA model and especially More's PA model (both of which include a tonal factor) lead to lower psychoacoustic annoyance at optimal rotor spacing than Zwicker's PA model. (iii) While Zwicker's and Di et al.'s PA models give the minimum value of psychoacoustic annoyance at rotor spacing z/D=0.2, the lowest psychoacoustic annoyance according to More's PA model is at z/D=0.35. This seems to be due to the higher contribution of the tonal factor in the PA model developed by More (see Fig. 6).

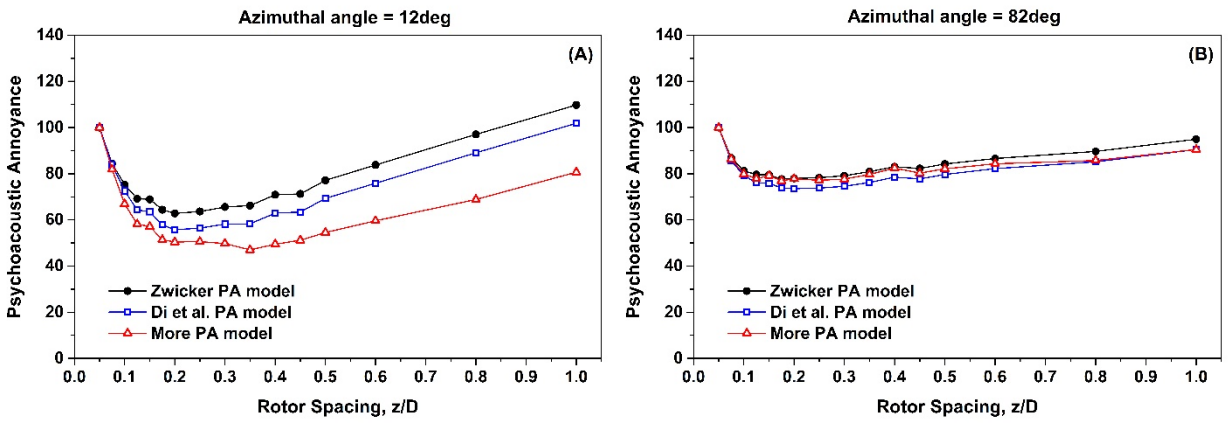

361

362 FIG. 5. (Color online). Psychoacoustic annoyance (PA) calculated with Zwicker's, Di et al.'s and
363 More's PA models as a function of rotor spacing, for azimuthal angle 12 deg (A) and 82 deg (B) with
364 a thrust setting of 10 N. Normalised to PA = 100 at z/d=0.05.

365 At 82 degrees, i.e. the emission angle with the lowest amplitude of potential field interaction tones,
366 it is observed that the three models implemented give similar values of PA (Fig. 5B). The PA model
367 developed by Di et al. (2016) gives the lowest values of PA among the three models used. The values
368 of PA calculated according to the model developed by More are higher than the values calculated with
369 Di et al.'s PA model for the rotor spacing range z/D=0.15-0.6. This seems to be due to the higher
370 contribution of the sharpness factor in the PA model developed by More (see Fig. 4F for sharpness
371 vs. rotor spacing). At this emission angle, the range of variation of PA as a function of rotor spacing
372 is significantly more reduced than at an emission angle of 12 degrees. This finding suggests that a
373 suboptimal rotor spacing between contra-rotating propellers can lead to a significant increase in PA
374 at emission angles in line to the rotor axis. These emission angles are typical for an observer on the
375 ground interacting with a hovering contra-rotating UAV.

376 Zwicker's and Di et al.'s PA models (Zwicker and Fastl, 1999; Di et al., 2016) were derived for a
377 series of mechanical sounds, and More (2011) modified Zwicker's PA model to account for
378 characteristics of fixed-wing aircraft noise. However, none of these PA models have been optimised

379 for propeller noise, and therefore might not be able to account for the complex perceptual interactions
380 between individual noise sources (e.g. tonal components, roughness due to interactions between
381 closely spaced tones, broadband noise in high frequency region due to unsteadiness in the wake,
382 propeller-turbulence interaction noise, etc.). This might lead to important uncertainty in the prediction
383 of PA with current models available. Furthermore, in the three PA models implemented in this work,
384 loudness is included as a first order term, and the other psychoacoustic metrics are just second order
385 factors. For this reason, the calculations of PA with these psychoacoustic models are mainly driven
386 by loudness, and the contribution of other psychoacoustic factors is quite reduced. Sharpness has
387 been found to be an important contributor to aircraft noise annoyance (Torija et al., 2019). Sharpness,
388 tonality and fluctuation strength were found to be important predictors of annoyance for rotorcraft-
389 like sounds (Krishnamurthy et al., 2018; Boucher et al., 2020). Roughness has been found, for instance,
390 an important factor to describing sound quality of electric motors (Mosquera-Sanchez et al., 2014;
391 Ercan, 2019). The relative contribution of psychoacoustic features to annoyance for propeller noise is
392 unknown. A process of listening tests and optimization of coefficients for psychoacoustic terms in
393 PA models, similar to the one carried out by More (2011) for fixed-wing aircraft, is needed for
394 propeller noise.

395 A recent study carried out by Gwak et al. (2020) has investigated the relationship between
396 psychoacoustic metrics and the annoyance reported for a range of hovering UAVs of varying size.
397 The authors found that the annoyance reported for medium and large drones is driven by loudness,
398 sharpness and fluctuation strength; they also found that the annoyance reported for small drones
399 cannot be explained by the three psychoacoustic metrics above, but tonality might play an important
400 role. Based on the β-coefficients of a linear regression model of the annoyance for medium and large
401 drones developed by Gwak et al. (2020, pp. 13), reported annoyance is mainly driven by loudness (β
402 = 0.908) and sharpness (β = 0.102) and fluctuation strength (β = 0.268) are second order contributors.

Further, the standardised β-coefficients of the linear regression model indicate that an increase of 0.516 loudness units (i.e. sones) is needed to increase the annoyance in 1 unit[1], while an increase of 9.902 sharpness units (i.e. acum) is needed for an increase in 1 unit of annoyance. Using the results of Gwak et al. (2020), the increase in the contribution of sharpness (relative lo loudness) needed in order for it to dominate the psychoacoustic annoyance calculation is unrealistic. Based on this, one could argue that the optimal rotor spacing, in terms of psychoacoustic annoyance, suggested in this paper is not subjected to specific models but a more general finding.

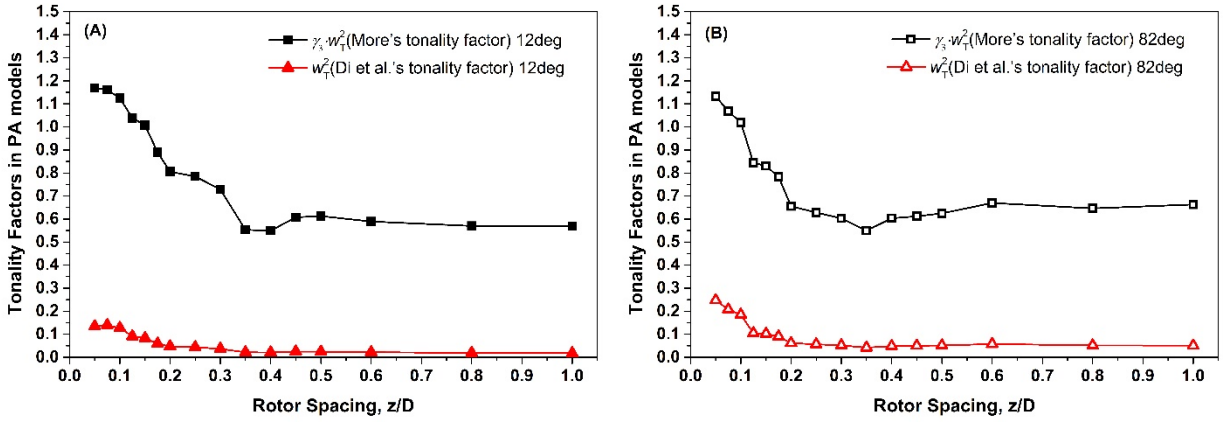

FIG. 6. (Color online). Di et al.'s tonality factor (w_T^2) and More's tonality factor ($\gamma_3 w_T^2$) in PA models as a function of rotor spacing, for azimuthal angle 12 deg (A) and 82 deg (B) with a thrust setting of 10 N.

Although the perceived roughness and impulsiveness might be a factor due to unsteady turbulence-propeller interaction noise, annoyance might be assumed to be primarily driven by perceived tonality in the region of optimal rotor spacing as shown in Figs. 4B and 5 (i.e. sound is eminently tonal in nature in this region due to the contribution of potential field interaction tones). Several studies on a variety of noise sources, such as mechanical ventilation systems (Lee, 2016) and aircraft noise (More and Davies, 2010) have suggested a combination of loudness and tonality factors

[1] Note that annoyance in Gwak et al. (2020) is assessed using a 11-point scale.

420 in multiple linear regression models as an accurate approach to predict annoyance. As seen in Fig. 6,
421 both the tonality factors derived by Di et al. (2016) and More (2011) (accounting for the combined
422 effect of loudness and tonality) suggest the optimal rotor spacing at $z/D \geq 0.35$ (note that the minimum
423 value of both tonality factors is at $z/D=0.35$). Figure 6 shows the Di et al.'s tonality factor squared
424 (eq. 5), and More's tonality factor squared (eq. 7) multiplied by $\gamma_3 = 1.25$ (to account for the total
425 contribution of tonality in More's PA model). This figure also shows that More's tonality factor
426 emphasises more the contribution of tonality in the PA model than Di et al.'s. The value of both
427 tonality factors as a function of rotor spacing demonstrates that More's factor is more sensitive to
428 variations in tonality, and therefore would lead to higher variation in PA for the same changes in
429 tonality.

430 Future work for the development of PA models for propellers, and especially contra-rotating
431 multiple blade propellers, will need to focus on psychoacoustic features such as perceived
432 impulsiveness caused by propeller-turbulence interaction, and perceived roughness and perceived
433 tonality of multiple tone complexes. Perceived roughness of superpositioned multiple pure tones (see
434 Fig. 3) differs from perceived roughness of amplitude modulated tones, even with similar modulation
435 strengths (Terhardt, 1974; Aures, 1985a). Perakis et al. (2013) found that the modulation index of an
436 amplitude modulated tone must be lowered by 2/3 to be perceived as equally rough as a pair of
437 superpositioned tones. This perceptual phenomenon should be taken into account when deriving a
438 fluctuation strength/roughness function accounting for the perceptual interaction effect of closely
439 spaced multiple tones. The perceived tonal strength of mechanical sounds containing series of
440 harmonic or inharmonic complex tones can adversely influence the perception of these sounds (Lee
441 et al., 2005). The prediction of annoyance from sounds containing multiple tone complexes requires
442 not only accounting for the tonality of the most prevailing tone and signal loudness, but also the
443 frequencies and the structure of the other tones in the noise signal (Lee and Wang, 2020).

Aures/Terhardt tonality model (Aures, 1985b) accounts for the presence of complex tones. However, Lee at al. (2005) found that Aures/Terhardt tonality model overestimates perceived tonality of complex tones. These authors modified Aures/Terhardt tonality with a factor accounting for the differences in tonality perception between harmonic complexes and single tones, and concluded that the perceived tonality of multiple tone complexes is a function of the pitch strength of the harmonic components. Therefore, pitch perception models, such as Terhardt's virtual pitch model (Terhardt et al., 1982a;b) should be taken into account when deriving a function accounting for the perceived tonality of complex tones in propeller noise.

IV. CONCLUSION

This paper presents the results of a psychoacoustic analysis carried out to investigate the optimal distance between contra-rotating propellers to minimise noise annoyance. On the basis of psychoacoustic annoyance, calculated with models available in the literature, it can be concluded that the optimal rotor axial separation distance for the contra-rotating propellers under study is at a range of z/D=0.2-0.4, instead of previously observed z/D=0.25 by Chaitanya et al. (2020) on the basis of overall sound power level. Similar optimal rotor spacing is found for azimuthal angles of maximum and minimum emission of potential field interaction tones, which are the highest contributors to the contra-rotating propellers sounds measured. These results are consistent with the rotor spacing with maximum aerodynamic efficiency for this contra-rotating system, measured at $z/D = 0.3$ by Chaitanya et al. (2020). Although the Aures/Terhardt tonality metric and More's and Di et al.'s tonality factors suggest an optimal rotor spacing at $z/D \geq 0.35$, the psychoacoustic annoyance as calculated with the three models implemented in this work significantly increases for rotor spacings over $z/D = 0.4$. Furthermore, a rotor separation over $z/D = 0.4$ might be more impractical from a construction perspective.

Below the optimal rotor spacing, the noise generation is dominated by potential field interactions between the two contra-rotating rotors, which is consistent with previous observations (McKay et al., 2019; Chaitanya et al., 2020). As the rotor spacing increases towards the optimum, the magnitude of these potential field interactions lessens significantly, and therefore a decrease in loudness is observed. As this source of noise is tonal in nature, tonality also drops significantly at the optimum rotor spacing. This decrease in tonality, and especially loudness, lead to a minimum in psychoacoustic annoyance. Fluctuation strength accounts for the slow amplitude modulation due to closely spaced potential field interaction tones, and therefore drops importantly as the amplitude of these interaction tones decays.

With increased rotor separation distances after optimum, interaction noise between contra-rotating rotors increases due to enhance turbulence-propeller interactions, and this leads to an increase in loudness. Furthermore, as this is unsteady broadband noise in nature, roughness and impulsiveness increase when rotors move apart. This suggests that the perceptual effect of propeller-turbulence interaction noise could be accounted for by roughness and/or impulsiveness metrics.

A special case takes place when calculating sharpness as a function of rotor spacing. Sharpness reaches the highest values at the optimal rotor spacing region. As potential field interaction tones, distributed evenly along low-to-mid frequencies, decays significantly at the optimal rotor separation distance, the centroid of the spectrum moves towards the high frequency region (i.e. the relative contribution of high frequency tonal and broadband noise increases). Under these conditions of more dominant high frequency noise components, the values of sharpness are consequently higher.

The approach described in this paper, based on psychoacoustic methods available in the literature, provides a more sophisticated and comprehensive analysis than traditional sound power level analyses to inform the optimal design of rotating systems for lowest noise annoyance. Compared to sound power level based assessments, the proposed method is able to account for the key psychoacoustic features highly correlated to noise perception (e.g. tonality, roughness). Appropriately accounting for

491 the perceptual effects of key psychoacoustic factors is crucial for the optimisation of designs for lower
492 noise impact on potential exposed communities. As observed in this paper, minor deviations from
493 the optimal design (in terms of rotor spacing) of contra-rotating propellers can lead to substantial
494 increase in noise annoyance at emission angles typical for an observer on the ground interacting with
495 a hovering UAV.

496 The three models implemented in this research gives the minimum psychoacoustic annoyance at
497 similar rotor spacings. Despite differences in tonality, these models are mainly driven by loudness.
498 Analysing findings of recent literature, the increase in the contribution (relative to loudness) of some
499 secondary factors (e.g. sharpness) required to become dominant for psychoacoustic annoyance might
500 be unrealistic. Based on the above, it could be argued that other psychoacoustic annoyance models
501 might also lead to the same conclusion in terms of optimum rotor spacing, and therefore, the results
502 of this paper are more general and no specific to the three annoyance models implemented. However,
503 this cannot be demonstrated without extensive testing, as it is uncertain whether these psychoacoustic
504 annoyance models provide an accurate picture of actual noise perception for propeller noise (and
505 specifically contra-rotating rotor noise). The relative contribution to noise annoyance of different key
506 psychoacoustic features in a variety of rotor noise must be investigated to derive psychoacoustic
507 annoyance models optimised for rotating systems.

508 Further work is recommended to aid the design of rotating systems for lowest noise impact: (1)
509 additional noise testing should be carried out to gather a comprehensive database with sound samples
510 of different blade geometries, thrust settings, emission angles and single vs. coaxial propellers; (2)
511 further analyses will include other psychoacoustic factors, such as impulsiveness, relative approach
512 and additional tonality models; and (3) extensive subjective testing should be conducted to identify
513 the psychoacoustic factors mainly driving rotor noise annoyance, refine or compute coefficients

514 accounting for their relative contribution to noise annoyance, and thus, develop psychoacoustic
515 annoyance models for rotor noise.

516 **ACKNOWLEGEMENTS**

517 The first author would like to acknowledge the financial support of the Royal Academy of
518 Engineering, United Kingdom (RF/201819/18/194). The authors would also like to thank Dr.
519 Mantas Brazinskas and Dr. Stephen Prior for their efforts in building this rig at the University of
520 Southampton. Dr Zhengguang Li would like to thank the funding of Natural Science Foundation of
521 Zhejiang University of Science and Technology (No. 2019QN15).

522 **REFERENCES**

523 Aerospace Technology Institute (ATI) (2019). Accelerating Ambition: Technology Strategy 2019.
524 Available at: https://www.ati.org.uk/media/siybi1mm/reduced-ati-tech-strategy.pdf (last
525 accessed: 07/04/2020)

526 Alexander, W.N., Whelchel, J., Intaratep, N. and Trani, A. (2019). "Predicting community noise of
527 sUAS." Proceedings of 25th AIAA/CEAS Aeroacoustics Conference, Delft, The
528 Netherlands.

529 Angerer, R., Erickson, R.A., and McCurdy, D.A. (1991). "Development of an annoyance model based
530 upon elementary auditory sensations for steady-state aircraft interior noise containing tonal
531 components." NASA technical report TM 104147.

532 Anghinolfi, D., Canepa, E., Cattanei, A., and Paoluci, M. (2016). "Psychoacoustic optimization of the
533 spacing of propellers, helicopter rotors, and axial fans." Journal of Propulsion and Power,
534 32(6), 1422-1432.

535 Aures, W. (1985a). "Ein Berechnungsverfahren der Rauhigkeit (A Calculation Method for
536 Roughness)." Acustica 58, 268–280.

Aures, W. (1985b). "Berechnungsverfahren für den sensorischen wohlklang beliebiger schallsignale" ("A procedure for calculating sensory pleasantness of various sounds."). Acta Acustica united with Acustica, 59(2):130-141, 1985.

Barbot, B., Lavandier, C., Cheminee, P. (2008). "Perceptual representation of aircraft sounds." Applied Acoustics, 69, 1003-1016.

Berckmans, D., Janssens, K., Van der Auweraer, H., Sas, P., and Desmet, W. (2008). "Model-based synthesis of aircraft noise to quantify human perception of sound quality and annoyance." Journal of Sound and Vibration, 311, 1175-1195.

Boucher, M., Krishnamurthy, S., Christian, A., and Rizzi, S.A. 2020. "Sound quality metric indicators of rotorcraft noise annoyance using multilevel regression analysis". Proc. Mtgs. Acoust. 36, 040004 (2019); doi: 10.1121/2.0001223

Brackley, M., and Pollock, C. (2000). "Analysis and reduction of acoustic noise from a brushless dc drive." IEEE Transactions on Industry Applications, 36(3), 772-777.

Brazinskas, M. (2019). "An empirical investigation into interference effects of small-scale rotors for use in vtol unmanned aircraft". PhD thesis, University of Southampton.

Cabell, R., Grosveld, F., and McSwain, R. (2016). "Measured noise from small unmanned aerial vehicles." Proceedings of NOISE-CON 2016, Vol. 252, Institute of Noise Control Engineering, Providence, RI, USA.

Chaitanya, P., Joseph, P., Prior, S. D., Parry, A. B. (2020). "On the optimum separation distance for minimum noise of contra-rotating propellers." Journal of Fluid Mechanics (Under review). The submitted version of the paper can be accessed upon request at: http://eprints.soton.ac.uk/id/eprint/444759

559 Christian, A.W. and Cabell, R. (2017). "Initial investigation into the psychoacoustic properties of small
560 unmanned aerial system noise." Proceedings of the 23rd AIAA/CEAS Aeroacoustics
561 Conference, AIAA Aviation Forum, Denver, USA.
562 Daniel, P. (2008). "Psychoacoustical roughness." In Havelock, D., Kuwano, S., and Vorlander, M.
563 (Ed.). Handbook of signal processing in acoustics, Vol. 1, pp. 263-275. New York, USA:
564 Springer.
565 Di, G-Q., Chen, X-W., Song, K., Zhou, B., and Pei, C-M. (2016). "Improvement of Zwicker's
566 psychoacoustic annoyance model aiming at tonal noises." Applied Acoustics 105:164-170.
567 DIN 45631/A1-2010. "Calculation of loudness level and loudness from the sound spectrum - Zwicker
568 method - Amendment 1: Calculation of the loudness of time-variant sound."
569 DIN 45692-2009. "Measurement technique for the simulation of the auditory sensation of sharpness."
570 Ercan, A. M. (2019). "Sound quality of small electric motors." Proceedings of InterNoise 2019,
571 Madrid, Spain.
572 Gwak, D.Y., Han, D., and Lee, S. (2020). "Sound quality factors influencing annoyance from hovering
573 UAV." Journal of Sound and Vibration, 115651.
574 HEAD Acoustics (2018). "Loudness and sharpness calculation." Technical Report Application Note
575 - 02/18
576 Heff, G.E. (1990). "Experimental performance and acoustic investigation of modern, counterrotating
577 blade concepts." NASA Contractor Report 185158.
578 Krishnamurthy, S.,Christian, A., and Rizzi, S. (2018). "Psychoacoustic test to determine sound quality
579 metric indicators of rotorcraft noise annoyance." Proceedings of Inter-Noise 2018 Impact of
580 Noise Control Engineering, Chicago, USA.

581 Krishnamurthy, S., Rizzi, S.A., Boyd Jr., D.D., and Aumann, A.R. (2018). "Auralization of rotorcraft
582 periodic flyover noise from design predictions." Proceedings of the AHS International 74th
583 Annual Forum & Technology Display, May 14-17, 2018, Phoenix, Arizona, USA.
584 Lee, K.H., Davies, P., and Surprenant, A.M. (2005). "Tonal strength of harmonic complex tones in
585 machinery noise." Journal of the Acoustical Society of America 118, 1921.
586 Lee, J. (2016). "The effects of tones in noise on human annoyance and performance." PhD
587 dissertation, University of Nebraska.
588 Lee, J., and Wang, L.M. (2020). "Investigating multidimensional characteristics of noise signals with
589 tones from building mechanical systems and their effects on annoyance." Journal of the
590 Acoustical Society of America 147, 108-124.
591 Lyon, R.H. (2003). "Product sound quality – from perception to design." Sound and Vibration, 37(3),
592 18-23.
593 McMullen, A.L. (2014). "Assessment of noise metrics for application to rotorcraft." Master's Thesis,
594 Purdue University.
595 Magliozzi, B., Hanson, D.B., and Amiet, R.K. (1991). "Propeller and propfan noise." In Harvey H.
596 Hubbard, editor, Aeroacoustics of Flight Vehicles: Theory and Practice: Volume 1: Noise
597 Sources, number NASA RP-1258, pages 1–64.
598 Marte, J. E. & Kurtz, D. W. (1970). "A review of aerodynamic noise from propellers, rotors, and lift
599 fans." NASA Technical Report NASA-32-7462.
600 McKay, R.S., Kingan, M.J. and Go, R. 2019. "Experimental investigation of contra-rotating multi-
601 rotor UAV propeller noise." Proceedings of ACOUSTICS 2019, Cape Schanck, Victoria,
602 Australia.

603 Mestre, V., Fidell, S., Horonjeff, R.D., Schomer, P., Hastings, A., Tabachnick, B.G., and Schmitz, F.A.
604 (2017). "Assessing Community Annoyance of Helicopter Noise." Washington, DC: The
605 National Academies Press. Available at: https://doi.org/10.17226/24948.
606 More, S, and Davies, P. (2010). "Human Responses to the Tonalness of Aircraft Noise." Noise
607 Control Engineering Journal 58.4, 420–440.
608 More, S. (2011). "Aircraft noise metrics and characteristics." PhD Thesis, Purdue University.
609 Mosquera-Sánchez J.A., Villalba, J., Janssens, K., and de Oliveira, L.P.R. (2014). "A multi objective
610 sound quality optimization of electric motor noise in hybrid vehicles." Proceedings of
611 International Conference on Noise and Vibration Engineering (ISMA 2014), Leuven, Begium.
612 Perakis, G.J., Flindell, I.H., and Self, R.H. (2013). "Toward Roughness as an additional metric for
613 aircraft noise containing multiple tones." Acta Acustica United with Acustica 99, 828-835.
614 Rizzi, S.A. (2016). "Toward reduced aircraft community noise impact via a perception-influenced
615 design approach." Proceedings of InterNoise 2016, Hamburg, Germany.
616 Rizzi, SA., Burley, C.L., and Thomas, R.H. (2016). "Auralization of NASA N+2 Aircraft Concepts
617 from System Noise Predictions." Proceedings of the 22nd AIAA/CEAS Aeroacoustics
618 Conference. Lyon, France.
619 Sottek, R. (1993). "Modelle zur Signalverarbeitung im menschlichen Gehör" ("Models for signal
620 processing in human hearing."). PhD thesis, RWTH Aachen.
621 Sottek, R., Vranken, P., and Busch, G. (1995). "A model for calculating impulsiveness" ("Ein Modell
622 zrur Berechnung der Impulshaltigkeit"). Proceedings of DAGA 95 (German Acoustical
623 Society Meeting), Saarbrücken, Germany.
624 Sottek, R., and Genuit, K. (2005). "Models of signal processing in human hearing". International
625 Journal of Electronics and Communications (AEU) 59, 157-165.

626 Stract, W. C., Knip, G., Weisbrich, A. L., Godston, J. and Bradley, E. (1981). "Technology and Benefits
627 of Aircraft Counter Rotation Propellers." NASA Technical Memorandum 82983. Available
628 at: https://ntrs.nasa.gov/archive/nasa/casi.ntrs.nasa.gov/19830002859.pdf (last accessed:
629 07/04/2020)
630 Terhardt, E. (1974). "On the perception of periodic sound fluctuations (roughness)." Acustica 30,
631 548-560.
632 Terhardt, E., Stoll, G., and Seewann, M. (1982a). "Pitch of complex signals according to virtual-pitch
633 theory: Tests, examples, and predictions." Journal of the Acoustical Society of America 71,
634 671-678.
635 Terhardt, E., Stoll, G., and Seewann, M. (1982b). "Algorithm for extraction of pitch and pitch salience
636 from complex tonal signals." Journal of the Acoustical Society of America 71, 679-688.
637 Tinney, C.E. and Sirohi, J. (2018). "Multirotor drone noise at static thrust." AIAA Journal, 56(7), 2816-
638 2826.
639 Torija, A.J., Roberts, S., Woodward, R., Flindell, I.H., McKenzie, A.R., and Self, R.H. (2019). "On the
640 assessment of subjective response to tonal content of contemporary aircraft noise." Applied
641 Acoustics, 146, 190-203.
642 Torija, A.J., Self, R.H., and Lawrence, J.L.T. (2019). "Psychoacoustic characterisation of a small fixed-
643 pitch quadcopter." In: Proceedings of InterNoise 2019, Madrid, Spain.
644 White, K., Bronkhorst, A.W., and Meeter, M. (2017). "Annoyance by transportation noise: the effects
645 of source identity and tonal components." Journal of the Acoustical Society of America, 141,
646 3137-3144.
647 Zwicker, E. and Fastl, H. (1999). "Psychoacoustics – facts and models." Berlin: Springer-Verlag.